arXiv:2409.02612v1 [astro-ph.SR] 4 Sep 2024

Observed Fluctuation Enhancement and Departure from WKB Theory in Sub-Alfvénic Solar Wind

David Ruffolo [ID],[1] Panisara Thepthong [ID],[2] Peera Pongkitiwanichakul [ID],[2] Sohom Roy [ID],[3]
Francesco Pecora [ID],[3] Riddhi Bandyopadhyay [ID],[4] Rohit Chhiber [ID],[3,5] Arcadi V. Usmanov [ID],[3,5]
Michael Stevens [ID],[6] Samuel Badman [ID],[6] Orlando Romeo [ID],[7] Jiaming Wang [ID],[3] Joshua Goodwill [ID],[3]
Melvyn L. Goldstein [ID],[8] and William H. Matthaeus [ID][3,9]

[1]*Department of Physics, Faculty of Science, Mahidol University, Bangkok 10400, Thailand*
[2]*Department of Physics, Faculty of Science, Kasetsart University, Bangkok 10900, Thailand*
[3]*Department of Physics and Astronomy, University of Delaware, Newark, DE 19716, USA*
[4]*Department of Astrophysical Sciences, Princeton University, Princeton, NJ 08544, USA*
[5]*Heliophysics Science Division, NASA Goddard Space Flight Center, Greenbelt, MD 20771, USA*
[6]*Center for Astrophysics, Harvard & Smithsonian, Cambridge, MA 02138, USA*
[7]*Department of Earth & Planetary Science and Space Sciences Laboratory, University of California at Berkeley, Berkeley, CA 94720, USA*
[8]*Space Science Institute, Boulder, CO 80301, USA*
[9]*Bartol Research Institute, University of Delaware, Newark, DE 19716, USA*

ABSTRACT

Using Parker Solar Probe data from orbits 8 through 17, we examine fluctuation amplitudes throughout the critical region where the solar wind flow speed approaches and then exceeds the Alfvén wave speed, taking account of various exigencies of the plasma data. In contrast to WKB theory for non-interacting Alfvén waves streaming away from the Sun, the magnetic and kinetic fluctuation energies per unit volume are not monotonically decreasing. Instead, there is clear violation of conservation of standard WKB wave action, which is consistent with previous indications of strong *in situ* fluctuation energy input in the solar wind near the Alfvén critical region. This points to strong violations of WKB theory due to nonlinearity (turbulence) and major energy input near the critical region, which we interpret as likely due to driving by large-scale coronal shear flows.

1. INTRODUCTION

An important historical view of the fluctuations observed in the solar wind, dating to the early days of space exploration, is that these are predominantly "fossil" Alfvén waves that propagate outward from the Sun with little interaction (Coleman Jr 1967; Belcher & Davis Jr. 1971). This places specific constraints on the properties of observed magnetic and velocity fluctuations (Hollweg 1974; Barnes 1979) and greatly simplifies many models of the interplanetary transport of fluctuations (Hollweg 1990; Verma & Roberts 1993; Squire et al. 2020; Fisk & Kasper 2020). Frequently the assumption of unidirectional propagation goes along with an assumption of small amplitude transverse Alfvén waves, often considered "slab-like" in that they vary along one coordi-

nate direction. In the case that the wavelength is small compared to the scale of variation of a weakly inhomogeneous background, the transport of small-amplitude (non-interacting) Alfvén waves is governed by WKB theory (Weinberg 1962; Parker 1965). The present paper delves into specific details regarding the applicability of WKB theory in the solar wind.

The transport of one-dimensional waves having arbitrary wave lengths was considered by Heinemann & Olbert (1980). Although this model is much simpler than the three dimensional (3D) model for turbulence transport (Zhou & Matthaeus 1989; Matthaeus et al. 1994a), it suffices to demonstrate that violations of WKB ordering produce coupling between inward- and outward-propagating fluctuations even when nonlinear effects are neglected. A more complete 3D transport model (Verma & Roberts 1993) permits varying cross-helicity and nonequipartition of velocity and magnetic fluctuation energy, but still neglects energy input and turbulent dissipation; this model found that the radial varia-

Corresponding author: David Ruffolo
david.ruf@mahidol.ac.th

tion of fluctuation energy departed only marginally from WKB solutions. An analysis of a broad range of solutions to *linear* transport equations for solar wind fluctuations was presented by Oughton & Matthaeus (1995). Later Zank et al. (1996) showed that a full set of turbulence transport equations including shear driving and von Karman MHD dissipation (Wan et al. 2012) also closely follows WKB radial energy profiles, whereas the same equations without shear driving do not. This indicates that observation of WKB-like radial energy profiles in the (super-Alfvénic) solar wind is not sufficient to conclude that WKB theory is valid. In fact, beyond this single issue, for super Alfvénic wind far outside the critical region, e.g., at 1 au, there are numerous observational findings that demonstrate convincingly that the assumptions and (other) consequences of WKB theory are inconsistent with observations (Matthaeus & Velli 2011).

The validity of WKB theory for the sub-Alfvénic corona is much less well determined in the existing literature. This paper deals with that issue.

On the theoretical side, the presence of a large Alfvén speed would seem to favor wave propagation effects and therefore the physics entailed by WKB theory. Indeed WKB and its close relatives (Heinemann & Olbert 1980) are often involved in descriptions of coronal phenomena (see, e.g., Raouafi et al. 2023). Fortunately the Parker Solar Probe mission, with its regular forays into the sub-Alfvénic corona (Chhiber et al. 2024), provides for the first time an opportunity for direct observational testing of the relevance of WKB theory below the critical region.

2. DATA AND ANALYSIS PROCEDURE

We employ Parker Solar Probe (PSP) data, mainly derived from publicly accessible data archives. We use magnetic field ($\mathbf{B}$) data from the flux-gate magnetometer of the PSP/FIELDS instrument suite (Bale et al. 2016)[1], downsampled to a frequency of 4 Hz. Solar wind proton velocity ($\mathbf{V}$) data obtained from moments of the particle velocity data, are from the Solar Probe ANalyzer for Ions (SPAN-i) instrument in the PSP/SWEAP instrument suite (Kasper et al. 2016)[2]. We use SWEAP data at the native cadence, which is most commonly 0.87 s, or 1/4 of that near perihelion passages.

In our analysis we address two major concerns with the quality of the SWEAP/SPAN datasets: 1) The SPAN-i instrument has a limited field of view (Kasper et al. 2016; Livi et al. 2022) meaning it often has incom-

plete sampling of proton velocity distribution functions (VDFs). The field of view constraints are most severe in the tangential direction (or close to φ in instrument coordinates; see Figure 2 of Livi et al. 2022). Nevertheless, if the peak of the VDF falls into the instrument field of view, then the velocity moment vector is typically quite accurate. We filter the velocity moment data via the 'EFLUX_VS_PHI' CDF variable in the SPAN-i L3 data. If the peak energy flux is located lower than 160° in instrument azimuthal coordinates, then the velocity moment is accepted as a "good measurement". This azimuthal cutoff is conservative in that it also rejects measurements where the shadow of the PSP spacecraft heat-shield may distort the peak location.

2) Due to the above concerns, and after considerable experimentation with different approaches, we adopt a hybrid procedure to secure required plasma (proton) number density measurements N_p. First, when it is available we associate N_p with the electron number density (n_e) obtained from quasi-thermal noise (QTN) electric field data from the FIELDS suite (Moncuquet et al. 2020). We adopt a simplified heuristic approach by Romeo et al. (2023) to determine the QTN electron number density for each orbit. This method calculates the number density within $5 - 10\%$ of the density estimates derived by Moncuquet et al. (2020). We then perform a final stage of filtering to achieve a continuous signal. An exception is that for PSP solar encounter E15, we use the QTN data directly from the Moncuquet et al. procedure[3]. For all of the PSP encounters considered here, E8 through E17, when QTN data are not available, we use n_p data from SPAN, provided that the criterion regarding resolution of the particle distribution is satisfied. The measured SPAN n_p is then multiplied by an empirical factor of 0.86 (derived by a comparison with n_e data at the times when SPAN is in the field of view) to arrive at a plasma density $N_p = 0.86n_p$. When available from either of these sources, the useful plasma density data N_p is downsampled (averaged) to 1-minute cadence. This provides a times series with resolution several times smaller than the typical correlation times during these encounters, thus enabling diagnostics that measure properties of the local turbulent fluctuations.

For each minute of the data, selected as described above, we derive an Alfvén speed, V_A, of the proton-dominated plasma from

$$V_A = \frac{\langle |\mathbf{B}| \rangle}{\sqrt{\mu_0 m_p \langle N_p \rangle}}, \tag{1}$$

---

[1] http://research.ssl.berkeley.edu/data/psp/data/sci/fields/l2/

[2] http://sweap.cfa.harvard.edu/pub/data/sci/sweap/

[3] https://research.ssl.berkeley.edu/data/psp/data/sci/fields/l3/rfs_lfr_qtn/

where $\langle|\mathbf{B}|\rangle$ is the mean magnitude of the magnetic field during that minute, $\langle N_p \rangle$ is the mean plasma (proton) number density, as described above, during that minute, and m_p is the proton mass. The Alfvén Mach number M_A is then calculated as

$$M_A = \frac{\langle V_R \rangle}{V_A}, \qquad (2)$$

the ratio of the mean proton radial velocity to the local Alfvén speed for that minute.

Also required for this analysis are derived measures of turbulent fluctuations, especially δB for the rms magnetic fluctuation. We use this case as an example. For each minute of the data $\mathbf{B}$, we find the mean magnetic field components $\langle B_i \rangle$. Then we determine $(\delta B_i)^2 = \langle B_i^2 \rangle - \langle B_i \rangle^2$ as the mean-squared fluctuation of each field component relative to its mean value, i.e., the variance of that component during the minute. Finally, $\delta B = \sqrt{\sum_{i=1}^{3}(\delta B_i)^2}$. An analogous procedure was used to determine the velocity component fluctuations δV_i for each minute of data.

Incorporating the proton density dataset prepared according to the above procedure, and in consultation with various members of the SWEAP instrument team, we prepared an updated time series of Alfvén speed and Alfvén Mach number (Eq. 2). This dataset differs from typical simpler analyses, including that used in our own recent work (Chhiber et al. 2024). Fortunately the differences are, on balance, fairly subtle, consisting mainly of nearly isolated short periods wherein use of the more primitive SPAN dataset produces "spikes" of low Alfvén Mach number due to density dropouts at heliodistances greater than $\sim 30~R_\odot$. Most of these disappear when the more completely analyzed density data is employed. Our compilation of PSP density data will be made public.

Using the refined Mach number data allows examination of scalings of magnetic fluctuations with respect to M_A and with respect to radius $r/R_\odot$ to be carried out for numerous PSP orbits. Here we show data from encounters E8 through E17. We also examine velocity fluctuation energy per unit volume by computing a closely related surrogate $\rho \delta V^2 \equiv \rho \delta V_R^2 + 2\rho \delta V_N^2$. Here δV^2 is computed from the radial velocity component variance δV_R^2 and twice the normal component variance δV_N^2, i.e., using δV_N^2 as a proxy for δV_T^2. This avoids use of the tangential velocity component, whose distribution is cut off in the +T direction by SPAN field of view effects (Badman et al. 2023). The use of the surrogate amounts to asserting that the velocity field fluctuations are axisymmetric about the radial direction (Oughton et al. 2015). The assumption of axisymmetric fluctuations

is supported by observations of magnetic fluctuations, e.g., in the present data set the average of $\delta B_N^2/\delta B_T^2$ is within 1% of unity, and previous observations from Mariner 4 (Belcher & Davis 1971) and from PSP (Ruffolo et al. 2020; Fargette et al. 2022; Chhiber 2022) found that tangential-like and normal-like perpendicular increments of $\mathbf{B}$ have similar variances, especially at lags of 60 s or less.

3. RESULTS: FLUCTUATION SCALING VERSUS ALFVÉN MACH NUMBER

Employing the data processing procedures outlined above, we have in hand data from ten PSP orbits that are suitable for quantifying the level of adherence to WKB theory expectations.

Central to this question are the variations of the solar wind fluctuation energy densities per unit volume; for convenience, we suppress the factor of two in the definition of energy density, using $\delta B^2/\mu_0$ or $\rho \delta V^2$. The evolution of energy density is shown in Figure 1. The top row is for the magnetic fluctuation energy and the bottom row is for flow velocity fluctuation energy. Alfvén Mach dependence is shown in the left column, and radial distance dependence on the right. The points are widely scattered but bin averages, shown by connected symbols (red), provide well-defined tendencies.

In the evolution of the solar wind, a basic expectation is that M_A increases with increasing distance r from the Sun, as the wind changes from sub-Alfvénic to super-Alfvénic. However, in Figure 1, there is a strong visual difference between the dependence of various quantities versus M_A or $r/R_\odot$. Partly this is because different streams of the solar wind evolve differently in M_A as a function of r, and according to global MHD simulations that include turbulence, M_A can be non-monotonic even for a single stream (Chhiber et al. 2022). Note that the implementation of the WKB approximation (Parker 1965; Barnes 1975) assumes a steady state, a radial mean field, and $B_0 \propto r^{-2}$, but does not specify the radial dependence of the density and therefore retains the flexibility that different solar streams can evolve similarly in M_A but differently versus r. Therefore, the WKB predictions for fluctuation energy density $\mathcal{E}$ can be expressed in terms of M_A, in particular as $\mathcal{E} \propto [M_A(M_A + 1)^2]^{-1}$ (Jacques 1978), and not in terms of r unless additional assumptions are imposed. In this sense, the dependence of solar wind fluctuation parameters on M_A is expected to be fundamental, and can be obscured when expressed in terms of r because of the different evolution of different solar wind streams. In Figure 1(a) and (c), the Alfvén Mach number dependence expected from standard WKB theory is suggested
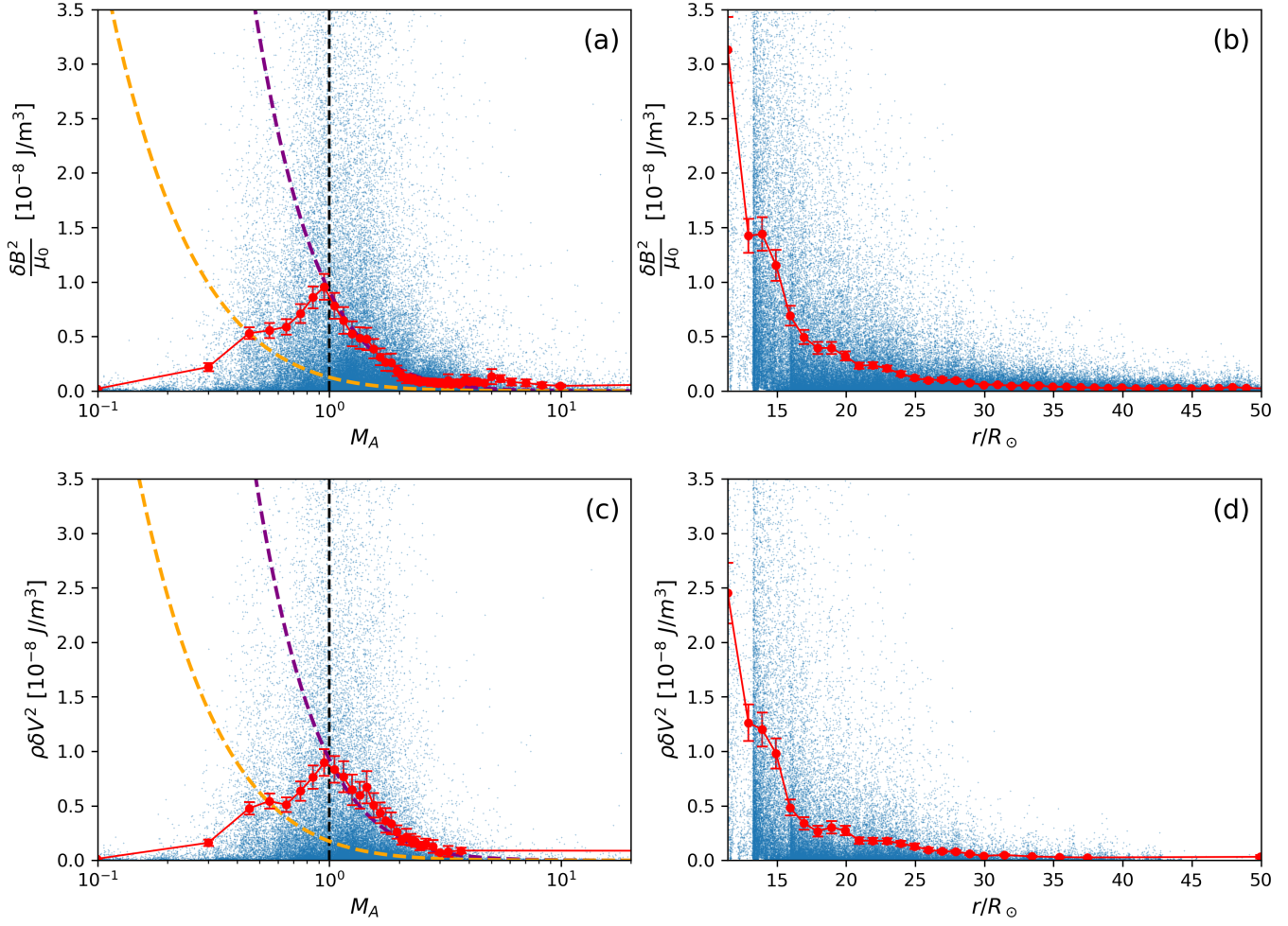
Figure 1. Solar wind fluctuation energy per unit volume vs. Alfvén Mach number M_A and radial distance r for PSP data during orbits 8 to 17. Each blue point shows a 1-minute-averaged value. Red circles indicate the average value in each bin of M_A having at least 100 data points, and the extent of vertical red lines indicates the standard deviation of data in that bin. Magnetic fluctuation energy per volume (a) $\delta B^2/\mu_0$ vs. M_A; and (b) vs. $r/R_\odot$. Velocity fluctuation energy per volume (c) $\rho\delta V^2$ vs. M_A; and (d) vs. $r/R_\odot$. M_A is computed using the density data set described in the text. Velocity fluctuation is computed only when SPAN-i data satisfy quality conditions described in the text. The evolutionary trend predicted from WKB theory for "fossil" Alfvénic fluctuations that propagate outward without interaction, $\mathcal{E} \propto [M_A(M_A + 1)^2]^{-1}$ (dashed curves in panels (a) and (c)), fails to explain the PSP data for sub-Alfvénic solar wind, i.e., for $M_A < 1$. The discrepancy implies that most solar wind fluctuation energy does not originate near the solar surface but rather is strongly enhanced *in situ* at $0.5 \lesssim M_A \lesssim 1$.

in dashed trend lines versus M_A, chosen to intersect the observed average energy per volume at values that facilitate comparison and discussion.

A familiar and not unexpected behavior of δB^2 versus $r/R_\odot$ is seen in Figure 1(b); it is essentially monotonically decreasing. However the behavior of δB^2 versus M_A in Figure 1(a) is less familiar in existing theoretical work on wave propagation and is not anticipated in WKB theory. In fact the WKB theory of fossil, non-interacting, outgoing Alfvénic fluctuations predicts a monotonic decrease of δB^2 as a function of M_A, with $\delta B^2 \propto [M_A(M_A + 1)^2]^{-1}$ as represented by the refer-

ence traces (dashed curves) in the Figure, which is not obtained for the PSP data as analyzed here.

Two rather distinct types of behavior are seen, separated by $M_A = 1$. Under sub-Alfvénic (coronal) conditions, with $M_A < 1$, one sees in the bin averages of δB^2 a regular increase when moving towards the Alfvén critical point $M_A = 1$. In the same region, the WKB reference traces are steeply declining. Since an inner boundary value for the WKB traces is arbitrary here, we chose the upper trace in panel (a) so that the reference curve coincides with the value of $\delta B^2/\mu_0$ at $M_A = 1$. It is then immediately apparent that the bin averaged δB^2 at superAlfvénic values of M_A actually are quite well fit

by the WKB profile. As striking as this agreement is, it is also not at all a surprise, since WKB-like behavior of δB^2 has been noted in data at 1 au in turbulence transport calculations when both shear driving and dissipation are included (Zank et al. 1996), and even in simpler models (Verma & Roberts 1993). However the extension of the curve that agrees so well with WKB at $M_A > 1$ is dramatically different from the averaged data values in the sub-Alfvénic region. Another WKB profile, the lower dashed curve in panel (a), passes through the bin averaged δB^2 data at around $M_A = 0.5$, but clearly fails to represent any aspect of the magnetic energy per unit volume in the sub-Alfvénic region.

Turning attention to the second row of panels in Figure 1, the quantity of interest changes to the kinetic energy per unit volume in the velocity fluctuations. The right panel (d) exhibits an essentially continuously decreasing value of $\rho \delta V^2$ as a function of distance $r/R_\odot$, qualitatively quite similar to the magnetic energy density in panel (b). The behavior of kinetic energy per volume $\rho \delta V^2$ vs. Alfvén Mach number also is very similar to that of δB^2 in panel (a): once again there are gross departures from WKB theory in the sub-Alfvénic coronal region, while the functional behavior in the super-Alfvénic region overlays nearly as well for $\rho \delta V^2$ vs. M_A as it did in panel (a) for δB^2 vs. M_A.
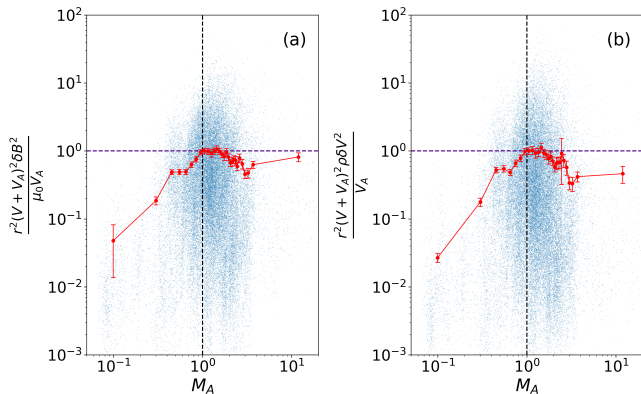
Figure 2. Quantities related to Alfvén wave action vs Alfvén Mach number M_A, expected to be conserved in WKB theory. (a) $r^2(V + V_A)^2 \delta B^2/(\mu_0 V_A)$ vs M_A, and (b) $r^2(V + V_A)^2 \rho \delta V^2/V_A$ vs M_A, evaluated here from PSP data, are not constant as function of M_A, except possibly for $1 < M_A < 2$. Solid (red) line is bin-averaged data. Vertical axes are normalized to the value at $M_A = 1$ (horizontal dark blue line). As a guide, vertical black dashed line at $M_A = 1$ indicates the Alfvén transition zone. In the sub-Alfvénic region ($M_A < 1$) these quantities are increasing, violating conservation of wave action and suggesting *in situ* fluctuation energy enhancement.

The evidence so far presented from PSP depicts significant departures from WKB profiles. Another perspective on this is obtained by examining the behavior of the *wave action* in a familiar standard form. In particular, assuming a radial mean field, non-interacting Alfvén waves in a weakly inhomogeneous medium, the conservation of mass flux and magnetic flux, and the absence of damping, one finds that (Jacques 1977)

$$\frac{r^2(V + V_A)^2 \mathcal{E}}{V_A} = const. \tag{3}$$

where $\mathcal{E} = \rho \delta V^2 = \delta B^2/\mu_0$ according to the equipartition of velocity and magnetic fluctuations for unidirectionally propagating Alfvén waves. This relation is usually called conservation of wave action, and is a central property of standard WKB as applied to the solar wind (Parker 1965; Barnes 1975). The same collection of data used above can be employed to evaluate the degree to which the wave action so defined is conserved in the PSP observations. This analysis is shown in Figure 2, showing scatter plots of the left hand side of Eq. (3) for $\mathcal{E} = \delta B^2/\mu_0$ (left panel) or $\rho \delta V^2$ (right panel), in each case *vs.* M_A. The red points are obtained by averaging the individual data values in bins containing at least 100 points. In the sub-Alfvénic range, wave action is seen to increase towards $M_A = 1$. For $M_A \gtrsim 2$ the magnetic wave action appears to decrease until about $M_A = 3$, possibly with near constant value thereafter. Similar behavior is observed for the velocity wave action in the right panel. Once again this demonstrates departures from WKB theory, at a level that should be viewed as significant.

Finally, in Figure 3 we examine the WKB assumption of equipartition by computing the behavior of the Alfvén ratio $r_A = \mu_0 \rho \delta V^2/\delta B^2$. This quantity is well understood to attain values less than unity (usually near $1/2$ at $r \sim 1$; orange dashed line) in the inertial range of turbulence as seen in solar wind observations and in MHD simulations (Matthaeus & Lamkin 1986). But in WKB theory it is expected to have a value of unity (blue dashed line). Here we test this prediction of wave theory. From Figure 3 we see that the average Alfvén ratio within bins in M_A is inconsistent with equipartition, with $r_A < 1$ at all values of M_A (except for a few bins with small sample sizes.) This is consistent with typical solar wind observations at larger heliocentric distances, near Earth and beyond (Matthaeus & Goldstein 1982; Bruno & Carbone 2013). Observation of systematic averages that deviate from equipartition represents another departure from WKB theory.

4. DISCUSSION AND SUMMARY
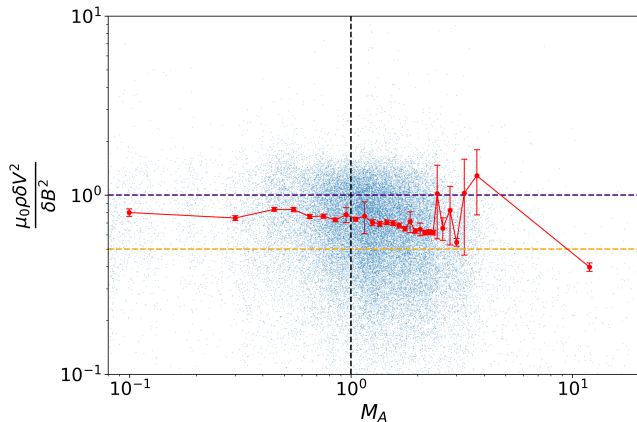
Figure 3. Alfvén ratio $r_A = \mu_0 \rho \delta V^2 / \delta B^2$ of solar wind fluctuation energies vs. Alfvén Mach number M_A. WKB theory for non-interacting fossil Alfvén waves predicts equipartition, i.e., $r_A = 1$. This PSP observation near the Sun is consistent with observations at greater distances that typically indicate $r_A < 1$. This can be understood in terms of turbulence effects (see, e.g., Matthaeus & Goldstein 1982; Matthaeus & Lamkin 1986; Thepthong et al. 2024). Orange dashed line marks 0.5 on vertical axis.

We have presented here what might be considered the first direct observational evidence that WKB wave propagation does not predict the radial evolution of MHD-scale fluctuations in the sub-Alfvénic coronal plasma. Note that our interpretation focuses on the increase of fluctuation energy far above the trend expected from WKB theory, as the Alfvén Mach number increases from $M_A \sim 0.5$ to $M_A \sim 1$, and does not rely on the more sparse data at $M_A < 0.5$. We say this is "direct" evidence because there is a well established class of models that require, at a fundamental level, non-WKB effects to produce coronal heating and solar wind acceleration. These include *reflection driven* and *wave-turbulence* models (Matthaeus et al. 1999; Cranmer et al. 2007; Breech et al. 2008; Verdini et al. 2010; van der Holst et al. 2014; Usmanov et al. 2018) that provide reasonable agreement with a variety of observed solar wind properties, even taking into account their subtle differences. Quite generally these models involve non-WKB transport (Zhou & Matthaeus 1989), including *leading order* production of "inward" fluctuations (meaning the minority cross-helicity or Elsässer species). The same models typically invoke a von Karman-style dissipation function that provides plasma heating due to nonlinear couplings and a turbulent cascade. The successes of these models in explaining observations throughout the heliosphere and in particular PSP observations (Adhikari et al. 2020; Chhiber et al. 2021) *indirectly* support the underlying assumptions of non-WKB transport. A summary of such observational departures

of super-Alfvénic wind from WKB expectations is given by (Matthaeus & Velli 2011).

The present direct observational evidence that WKB theory is not valid in the sub-Alfvénic corona, along with the supporting indications based on successes of non-WKB transport models, lead to the conclusion that WKB, as a fundamental theoretical building block, is not defensible, either in the corona or in the super-Alfvénic solar wind. It is at best a crude approximation and one that misses numerous important observed phenomena. Furthermore, this shows that non-interacting fossil fluctuations that propagate outward from the Sun should rapidly lose energy with increasing M_A and therefore represent at most a small portion of the total fluctuation energy even at the Alfvén critical region, which typically occurs at $r = 15$ to $20 R_\odot$.

There do remain nevertheless numerous references in the literature to arguments based on WKB that are purported to explain coronal phenomena. Perez & Chandran (2013) use WKB to demonstrate the validity of their coronal model. Squire et al. (2020) attribute the radial behavior of coronal fluctuations to WKB physics. In major recent reviews of PSP observations (e.g., Raouafi et al. 2023) some authors describe alternative models for explaining the occurrence of "switchbacks" in which the radial magnetic field B_R varies strongly or temporarily reverses in sign. A number of these models, but not all, depend on WKB-based reasoning. It would be an overreach to presume that all such applications of WKB can be discarded as a conceptual elements in constructing physical models. The theory still can occupy a role as an interesting limiting idealized case. It also can happen that WKB-like behavior emerges somewhat fortuitously, in a more complex scenario, as suggested by Verma & Roberts (1993) in a dissipationless model, and as shown to emerge in a balance between dissipation and forcing by Zank et al. (1996).

It is useful at this point to revisit the importance of the paper by Heinemann & Olbert (1980). This seminal work quantified the presence of non-WKB coupling between upward- and downward-traveling one-dimensional small amplitude waves, a type of "reflection" caused by spatial variations of Alfvén speed (or density). This is an antecedent of the more complete "mixing" term described by Zhou & Matthaeus (1989) and later suggestively called the MECS terms for "Mixing, Expansion, Compression and Shear" by Zank et al. (1996). In Heinemann & Olbert (1980), reflection occurs when the wave frequency become low enough that the WKB scale expansion begins to fail. This is enough to introduce some non-WKB effects, but having a long wavelength is

clearly not the only way to enter the non-WKB regime. The distribution of wavevectors in three dimensions and nonlinearity are both also important, or even dominant factors. In the nonlinear regime, fluctuations no longer obey dispersion relations derived in linear wave theory. When wave packets with inward- and outward-type polarizations (Elsässer packets in z^+ and z^-) have high enough frequency difference, there is no coupling and WKB is enforced. This property is shown in detail in Matthaeus et al. (1994b). In contrast, for strong turbulence, almost all Fourier amplitudes (in wave vector space) have significant power at low, nearly zero frequency (Dmitruk & Matthaeus 2009). The frequency *difference* of these colliding fluctuations is so low that WKB cannot be enforced. Reflection, and other MECS effects can then occur. Heinemann and Olbert describe one route to such low frequency differences, but strong turbulence, as well as quasi-two dimensional (2D) turbulence (with very long parallel wavelength) are equally effective, and perhaps more realistic elements of inertial range solar wind and coronal fluctuations.

Another interesting element in Heinemann & Olbert (1980) is the derivation of a conserved *total* wave action that applies to their small amplitude one dimensional case when when WKB ordering is not enforced and oppositely traveling wave packets are coupled by reflection, but not by local turbulence. It may be possible to derive a more general conservation law of this type when considering the full structure of the mixing terms in the linear non-WKB transport equations (see Matthaeus et al. 1994b; Oughton & Matthaeus 1995). Such a generalized conservation law may exhibit an inflection point at $M_A = 1$, as seen in the Heinemann and Olbert case, due to the change in the net group velocity (including the solar wind speed) of inward-propagating waves, from propagation toward $-\hat{r}$ for $M_A < 1$ to $+\hat{r}$ for $M_A > 1$. This might help explain the inflection at $M_A = 1$ as seen from the observations in our Figure 1.

It should be understood that the mixing terms are of crucial importance in causing violations of the WKB expansion. But the same terms are also responsible for triggering turbulent cascades in MHD-like plasma flows including those in the corona and solar wind. The turbulence, once present, also produces the broad range of frequencies at each wavelength that prohibits the occurrence of WKB ordering. But another significant effect of the mixing/MECS terms in non-WKB transport is the *production* of fluctuation energy. This can occur by the conservative exchange of energy from large scale shears (or magnetic shears) into small-scale fluctuations.

This, in outline, is the way that nonlinear Kelvin-Helmholtz rollups and mixing layers in hydrodynamics lead to enhanced turbulence. An analogous pathway for tapping coronal shear flows (DeForest et al. 2018) to form MHD scale rollups and "switchbacks" was proposed by Ruffolo et al. (2020) to occur near and outside the $M_A \sim 1$ transition region. Indeed the latter work predicted that sub-Alfvénic solar wind (which was not yet observed at that time) should have much weaker fluctuation energy, a prediction that we validate here. It is possible that the apparent buildup of fluctuation energy that we document here, as $M_A = 1$ is approached from below, may represent the onset of this energy exchange from coronal shears. Observations also indicate that the actual rollups/switchbacks occur in a more fully developed state at $M_A > 1$ (Bandyopadhyay et al. 2022; Pecora et al. 2022; Jagarlamudi et al. 2023). Further study will be needed to more fully understand the physics of this fascinating region of the corona and solar wind near the Alfvén critical zone (Chhiber et al. 2022; Cranmer et al. 2023).

REFERENCES

Adhikari, L., Zank, G. P., & Zhao, L. L. 2020, ApJ, 901, 102, doi: 10.3847/1538-4357/abb132

Badman, S. T., Stevens, M. L., Paulson, K. W., et al. 2023, in AGU Fall Meeting Abstracts, Vol. 2023, SH33B–01

Bale, S. D., Goetz, K., Harvey, P. R., et al. 2016, Space science reviews, 204, 49-82, doi: 10.1007/s11214-016-0244-5

Bandyopadhyay, R., Matthaeus, W., McComas, D., et al. 2022, The Astrophysical journal letters, 926, L1

Barnes, A. 1975, Advances in Electronics and Electron Physics, 36, 1, doi: 10.1016/S0065-2539(08)61117-8

Barnes, A. 1979, in Solar System Plasma Physics, vol. I, ed. E. N. Parker, C. F. Kennel, & L. J. Lanzerotti (Amsterdam: North-Holland), 251

Belcher, J. W., & Davis, Leverett, J. 1971, Journal of geophysical research, 76, 3534-3563, doi: 10.1029/ja076i016p03534

Belcher, J. W., & Davis Jr., L. 1971, J. Geophys. Res., 76, 3534

Breech, B., Matthaeus, W. H., Minnie, J., et al. 2008, J. Geophys. Res., 113, doi: 10.1029/2007JA012711

Bruno, R., & Carbone, V. 2013, Living Reviews in Solar Physics, 10, 2, doi: 10.12942/lrsp-2013-2

Chhiber, R. 2022, ApJ, 939, 33. doi:10.3847/1538-4357/ac9386

Chhiber, R., Matthaeus, W. H., Usmanov, A. V., Bandyopadhyay, R., & Goldstein, M. L. 2022, MNRAS, 513, 159, doi: 10.1093/mnras/stac779

Chhiber, R., Usmanov, A. V., Matthaeus, W. H., & Goldstein, M. L. 2021, The Astrophysical Journal, 923, 89

Chhiber, R., Pecora, F., Usmanov, A. V., et al. 2024, MNRAS, 533, L70, doi: 10.1093/mnrasl/slae051

Coleman Jr, P. J. 1967, Planetary and Space Science, 15, 953

Cranmer, S. R., van Ballegooijen, A. A., & Edgar, R. J. 2007, Astrophys. J. Suppl. Ser, 171, 520, doi: 10.1086/518001

Cranmer, S. R., Chhiber, R., Gilly, C. R., et al. 2023, Solar Physics, 298, 126

DeForest, C. E., Howard, R. A., Velli, M., Viall, N., & Vourlidas, A. 2018, ApJ, 862, 18, doi: 10.3847/1538-4357/aac8e3

Dmitruk, P., & Matthaeus, W. H. 2009, Physics of Plasmas, 16, 062304, doi: 10.1063/1.3148335

Fargette, N., Lavraud, B., Rouillard, A. P., et al. 2022, A&A, 663, A109. doi:10.1051/0004-6361/202243537

Fisk, L. A., & Kasper, J. C. 2020, ApJL, 894, L4, doi: 10.3847/2041-8213/ab8acd

Heinemann, M., & Olbert, S. 1980, J. Geophys. Res., 85, 1311, doi: 10.1029/JA085iA03p01311

Hollweg, J. V. 1974, J. Geophys. Res., 79, 1539

—. 1990, J. Geophys. Res., 95, 14 873

Jacques, S. A. 1977, Astrophys. J., 215, 942

Jacques, S. A. 1978, ApJ, 226, 632, doi: 10.1086/156647

Jagarlamudi, V. K., Raouafi, N. E., Bourouaine, S., et al. 2023, ApJL, 950, L7, doi: 10.3847/2041-8213/acd778

Kasper, J. C., Abiad, R., Austin, G., et al. 2016, Space science reviews, 204, 131-186, doi: 10.1007/s11214-015-0206-3

Livi, R., Larson, D. E., Kasper, J. C., et al. 2022, ApJ, 938, 138, doi: 10.3847/1538-4357/ac93f5

Matthaeus, W. H., & Goldstein, M. L. 1982, J. Geophys. Res., 87, 6011, doi: 10.1029/JA087iA08p06011

Matthaeus, W. H., & Lamkin, S. L. 1986, The Physics of fluids, 29, 2513, doi: 10.1063/1.866004

Matthaeus, W. H., Oughton, S., Pontius, D., & Zhou, Y. 1994a, J. Geophys. Res., 99, 19 267

Matthaeus, W. H., & Velli, M. 2011, Space Sci. Rev., 160, 145, doi: 10.1007/s11214-011-9793-9

Matthaeus, W. H., Zank, G. P., Oughton, S., Mullan, D. J., & Dmitruk, P. 1999, Astrophys. J., 523, L93

Matthaeus, W. H., Zhou, Y., Zank, G. P., & Oughton, S. 1994b, J. Geophys. Res., 99, 23 421

Moncuquet, M., Meyer-Vernet, N., Issautier, K., et al. 2020, The Astrophysical journal. Supplement series, 246, 44, doi: 10.3847/1538-4365/ab5a84

Oughton, S., & Matthaeus, W. H. 1995, J. Geophys. Res., 100, 14 783

Oughton, S., Matthaeus, W. H., Wan, M., & Osman, K. T. 2015, Philosophical Transactions of the Royal Society A, 373, 20140152, doi: 10.1098/rsta.2014.0152

Parker, E. N. 1965, SSRv, 4, 666, doi: 10.1007/BF00216273

Pecora, F., Matthaeus, W. H., Primavera, L., et al. 2022, The Astrophysical Journal Letters, 929, L10

Perez, J. C., & Chandran, B. D. G. 2013, The Astrophysical Journal, 776, 124, doi: 10.1088/0004-637X/776/2/124

Raouafi, N. E., Matteini, L., Squire, J., et al. 2023, Space Science Reviews, 219, 8

Romeo, O., Braga, C., Badman, S., et al. 2023, The Astrophysical Journal, 954, 168, doi: https://doi.org/10.3847/1538-4357/ace62e

Ruffolo, D., Matthaeus, W. H., Chhiber, R., et al. 2020, ApJ, 902, 94, doi: 10.3847/1538-4357/abb594

Squire, J., Chandran, B. D. G., & Meyrand, R. 2020, ApJL, 891, L2, doi: 10.3847/2041-8213/ab74e1

Thepthong, P., Pongkitiwanichakul, P., Ruffolo, D., et al. 2024, ApJ, 962, 37, doi: 10.3847/1538-4357/ad1592

Usmanov, A. V., Matthaeus, W. H., Goldstein, M. L., & Chhiber, R. 2018, Astrophys. J., 865, 25, doi: 10.3847/1538-4357/aad687

van der Holst, B., Sokolov, I. V., Meng, X., et al. 2014, Astrophys. J., 782, 81, doi: 10.1088/0004-637X/782/2/81

Verdini, A., Velli, M., Matthaeus, W. H., Oughton, S., & Dmitruk, P. 2010, Astrophys. J. Lett., 708, L116, doi: 10.1088/2041-8205/708/2/L116

Verma, M. K., & Roberts, D. A. 1993, J. Geophys. Res., 98, 5625

Wan, M., Oughton, S., Servidio, S., & Matthaeus, W. H. 2012, J. Fluid Mech., 697, 296, doi: 10.1017/jfm.2012.61

Weinberg, S. 1962, Phys. Rev., 126, 1899

Zank, G. P., Matthaeus, W. H., & Smith, C. W. 1996, J. Geophys. Res., 101, 17093, doi: 10.1029/96JA01275

Zhou, Y., & Matthaeus, W. H. 1989, Geophysical Research Letters, 16, 755